

Electron Paramagnetic Resonance and Scanning Tunneling Microscopy Investigations on the Formation of F^+ and F^0 Color Centers on the Surface of Thin MgO(001) Films

Martin Sterrer,* Esther Fischbach, Markus Heyde, Niklas Nilius, Hans-Peter Rust, Thomas Risse, and Hans-Joachim Freund

Department of Chemical Physics, Fritz-Haber-Institut der Max-Planck-Gesellschaft, Faradayweg 4-6, D-14195 Berlin, Germany

Received: January 25, 2006; In Final Form: March 10, 2006

The formation of surface color centers (F_S centers) by electron bombardment of thin MgO(001) films is investigated using electron paramagnetic resonance and low-temperature scanning tunneling microscopy. At low electron doses both techniques indicate the formation of singly occupied color centers (F_S^+), whereas at high electron doses the doubly occupied type (F_S^0) is dominant. It is suggested that with increasing electron dose F_S^+ centers are transformed into F_S^0 . Tunneling spectra of individual F_S^0 centers reveal a large distribution of energetic positions of occupied and unoccupied states, which is caused by local variations of the coordination number of the defects and explains the broad signals usually detected with integrating spectroscopic techniques.

Introduction

In this study we present a comparative electron paramagnetic resonance (EPR) and scanning tunneling microscopy (STM) study on the formation of surface color centers by electron bombardment of MgO(001) thin films. The investigation of charged point defects on the surface of MgO has recently gained attention because of their importance as nucleation sites as well as charge donors for adsorbed metal atoms and clusters. In particular, their effect on Au atoms and clusters has been studied both experimentally and theoretically.^{1–4} In MgO, color centers or F centers are constituted by electrons trapped in anion vacancies (F_S^{2+}) or related oxygen-deficient sites.⁵ Several different surface sites, e.g., oxygen vacancies on terraces, steps, and corners, as well as divacancies and morphological sites such as kinks and reverse corners, are capable of trapping electrons,^{6–9} which results in a manifold of defects with different electronic properties that are hard to distinguish experimentally. This situation is further complicated by the fact that color centers in MgO exist in two different charged states: singly occupied F centers (F_S^+) and doubly occupied F centers (F_S^0). Apart from the large amount of studies on the characterization of so-called $F_S^+(H)$ centers, i.e., color centers with a neighboring OH group, on MgO powders,^{10,11} only little information about the existence and properties of color centers located on single-crystalline surfaces has been available up to now. The most reliable way to create F centers on thin MgO films was found to be by electron bombardment. One suggested mechanism involves a two-step Auger deexcitation which triggers the desorption of oxygen atoms to form a doubly occupied F_S^0 center.¹² The electronic properties of the defects created in this way were studied by metastable impact electron spectroscopy (MIES) and electron energy loss spectroscopy (EELS).^{12–14} With MIES an occupied state located 2 eV above the valence band onset of MgO was assigned to the electronic ground state of color centers. Electronic transitions of color centers in the range between 1 and 3.5 eV were observed with EELS and, in

comparison with theoretical calculations, attributed to doubly occupied color centers in different surface locations.¹² A simple kinetic model including both the creation and annihilation of these centers was derived to explain the electron dose-dependent evolution of the EELS signal.

In recent studies, however, we could show by EPR and STM that also F_S^+ centers are present on the surface of thin MgO films.^{15,16} To gain more insight into the formation of F_S^+ centers during electron bombardment of the MgO surface, we present in this study EPR and STM results on the electron dose dependence of F_S^+ center formation on thin MgO films. We show that at low electron doses exclusively F_S^+ centers are formed, which, at increasing electron dosage, are transformed into F_S^0 centers. With scanning tunneling spectroscopy (STS), we probe both the occupied and the unoccupied states of the F_S^0 defects within the band gap of MgO. An analysis of a large number of individual color centers in terms of these states allows understanding of the line width usually observed with integrating spectroscopic methods.

Experimental Methods

Experiments were performed in two separate UHV chambers equipped with standard parts for substrate cleaning and thin film preparation. For EPR experiments, MgO thin films of typically 20 monolayer thickness were grown on Mo(001). The Mo substrate was cleaned by oxidation (1×10^{-6} mbar of O_2) at 1500 K and subsequent flashes to 2300 K. MgO was deposited by reactive deposition of Mg in oxygen¹⁷ (1×10^{-6} mbar) at a substrate temperature of 600 K and a deposition rate of 1 monolayer (ML) of MgO/min. EPR measurements were carried out at room temperature under UHV conditions. Typically 200 scans were accumulated to obtain a reasonable signal-to-noise ratio. STM experiments were performed in a custom-built low-temperature STM instrument operated at 5 K. Here, Ag(001) was used as the substrate, which was cleaned by repeated sputter (Ar^+)–anneal (700 K) cycles. Thin MgO films (4 MLs) were grown as described above at a substrate temperature of 550 K and a deposition rate of 0.75 ML of MgO/min. To create surface color centers, the MgO film was bombarded with electrons of

* To whom correspondence should be addressed. E-mail: sterre@fhi-berlin.mpg.de. Phone: +49 30 8413 4112. Fax: +49 30 8413 4105.

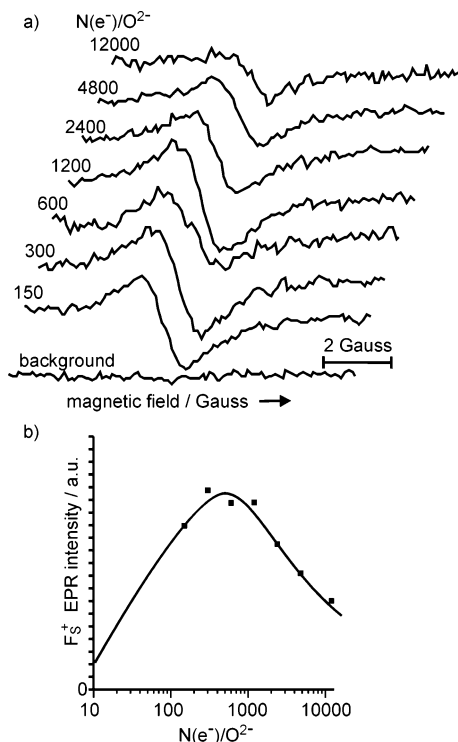


Figure 1. (a) EPR spectra of a 20 ML MgO(001) film recorded after preparation (lowest spectrum) and after electron bombardment with $E = 100$ eV and increasing electron dosage as indicated. (b) Semilogarithmic plot of the F_s^+ EPR peak-to-peak intensity depending on the electron dose.

100 eV energy at room temperature from a filament. The electron dosage was varied via the time of exposure at fixed energy and current and is given in units of electrons per surface oxygen ion (e^-/O^{2-}).

The use of two different substrates, Mo(001) and Ag(001), in these experiments is justified by the comparable surface morphologies of MgO films with the thicknesses indicated above. For STM experiments, Ag(001) is better suited because of the smaller lattice mismatch, which, at small film thicknesses of typically 3–4 MLs, results in films of better quality as compared to Mo(001).^{18,19} On the other hand, CO adsorption and LEED experiments have proven that MgO films of typically 10–30 ML thickness grown on Mo(001) exhibit extended terraces with only a small amount of defects.^{20,21} Furthermore, using Mo(001) as the substrate allows for thermal annealing of the MgO film to high temperature to improve the film quality. It has been reported that during high-temperature annealing defects are formed, which have been assigned to color centers.²² For an annealing temperature of 1200 K used here, no spectroscopic evidence for defect formation was found.

Results

In Figure 1a we report EPR spectra of a 20 ML thick MgO(001) film after electron bombardment with an energy of 100 eV at different electron doses. The lower curve gives the background spectrum of the freshly prepared MgO film, which shows that the pristine film contains no detectable amount of F_s^+ centers (within the detection limit of our EPR setup, this means $c(F_s^+) \leq 7 \times 10^{11} \text{ cm}^{-2}$).

After electron bombardment a resonance line around the free spin value ($g_e = 2.0023$) appears. Under the given measurement conditions (magnetic field direction perpendicular to the surface normal), the resonance line is almost symmetric. It has been

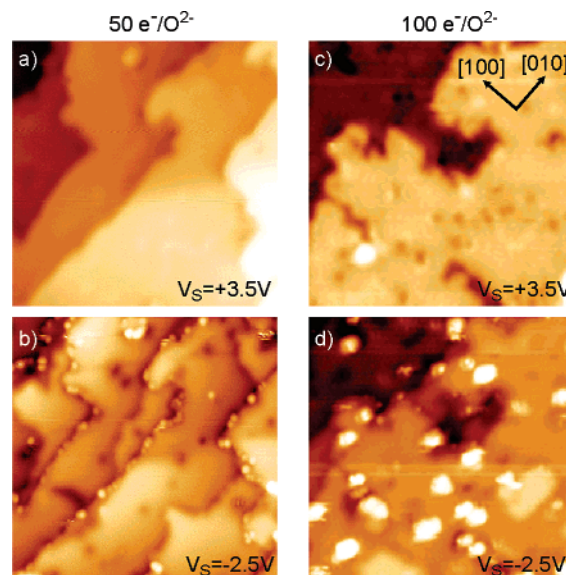


Figure 2. STM images (30×30 nm) of a 4 ML MgO(001) film grown on Ag(001) after bombardment with low (a, b) and high (c, d) electron doses. (a) and (c) were obtained at a sample bias of $V_s = +3.5$ V, and (b) and (d) at $V_s = -2.5$ V.

shown in a previous study that by varying the angle between the surface normal and magnetic field the resonance line undergoes slight changes both in line shape and in resonance position. From a theoretical analysis this signal was attributed to F_s^+ centers located on edges of MgO islands,¹⁵ in agreement with calculated EPR parameters.²³ The surface nature of these centers has been verified by their complete disappearance after addition of molecular oxygen. Already after bombardment with a low electron dosage ($150 e^-/\text{O}^{2-}$), an intense EPR signal due to F_s^+ centers is observed on the MgO thin films. The signal intensity increases slightly up to an electron dosage of 300–1000 e^-/O^{2-} and decreases again for higher exposures. It has to be noted that the EPR line shape and position do not change significantly in a series of this experiment, indicating no changes in the nature of the underlying defect. In Figure 1b, the peak-to-peak value of the F_s^+ EPR intensity is displayed as a function of the electron dosage according to Figure 1. This plot indicates a maximum for F_s^+ color center density at an electron exposure of around 800 e^-/O^{2-} . On the logarithmic scale of this plot the decrease of the F_s^+ concentration at higher electron dosage is linear, indicating first-order kinetics for the decay of F_s^+ centers in this regime.

In addition to the EPR experiment described above, which is sensitive to F_s^+ centers only, the formation of both F_s^+ and F_s^0 centers has been investigated with STM as a function of electron dosage. F_s^+ and F_s^0 centers are distinguishable in STM by their appearance in topographic images as well as by their different spectroscopic signatures.¹⁶ Defects associated with F_s^+ centers appear as dim features at negative sample bias and exhibit a defect state about 2 eV above the valence band onset. F_s^0 centers, on the other hand, give rise to bright protrusions at both negative and positive sample bias and two energy levels, one below and one above the Fermi energy, respectively.

In Figure 2 we report STM images at two different bias conditions of 4 ML thin MgO films deposited on Ag(001) that have been exposed to electron doses of 50 and 100 e^-/O^{2-} , respectively. At a bias voltage V_s of +3.5 V (Figure 2a,c) the morphology of the respective surface area is imaged.¹⁹ Defects corresponding to color centers are visible at a negative bias voltage of -2.5 V (Figure 2b,d).¹⁶ After exposure to 50 e^-/O^{2-}

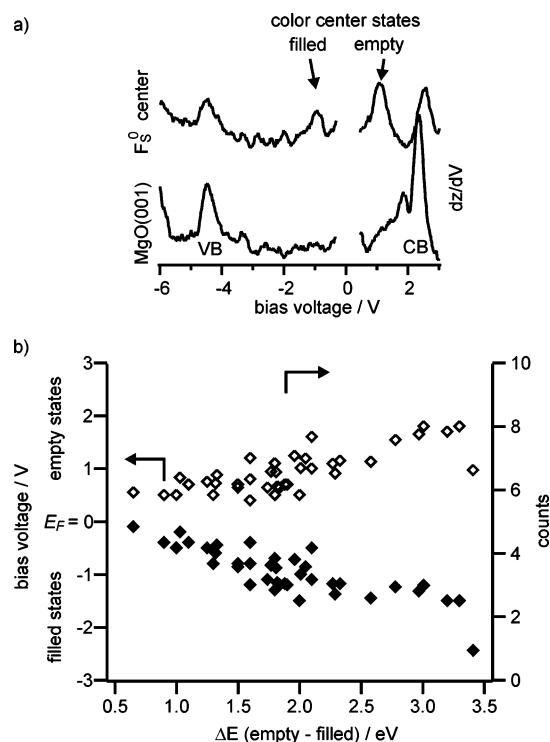


Figure 3. (a) dI/dV spectra obtained on the regular MgO(001) terrace (lower trace) and an F_s^0 defect (upper trace) on 4 ML MgO(001)/Ag-(001). (b) Pairs of filled and empty state energetic positions for an ensemble of F_s^0 defects and occurrence of defects with a specific energy difference between empty and filled states.

small protrusions are imaged at negative V_s in addition to the features of the MgO film (Figure 2b). These protrusions were previously assigned to F_s^+ centers.¹⁶ In accordance with EPR results the F_s^+ defects are located predominantly on the edges of MgO islands. (From Figure 2b we can estimate a concentration of about 2×10^{12} F_s^+ centers/cm², which is in the same range as the concentration of F_s^+ centers derived from the intensity of the EPR signals.) At this electron dosage almost no F_s^0 centers are observed in STM images. The situation is different when a higher electron dosage ($100 \text{ e}^-/\text{O}^{2-}$, Figure 2d) is applied. In Figure 2d both small protrusions corresponding to F_s^+ centers and bright spots indicative of F_s^0 centers are distinguishable.

As already mentioned above, tunneling spectra of color centers provide information about the energetic position of defect states as illustrated in Figure 3a. The lower spectrum in Figure 3a corresponds to the electronic states of the regular MgO(001) terrace. In agreement with previous studies we observe the onset of the conduction band at a bias voltage of about +2 V and the valence band onset at $V_s = -4.5 \text{ V}$.^{19,24} Between these two energies, no electronic states were observed. A spectrum taken on top of a F_s^0 defect (upper spectrum in Figure 3a), on the other hand, shows two peaks within the band gap of the MgO thin film. We assign the peak located below the Fermi energy of the Ag substrate as arising from the occupied F_s^0 color center states and the one above E_F as being due to the first unoccupied state of the color center defect. The position of these peaks is in accordance with calculated ground-state energy levels of color centers on the MgO surface.¹⁶

We have collected tunneling spectra of F_s^0 centers on different areas of an electron-bombarded MgO film. In Figure 3b the energy positions of the two states are plotted against the energy difference for a large set of defects. It is clearly seen that the position of both states varies considerably within the ensemble,

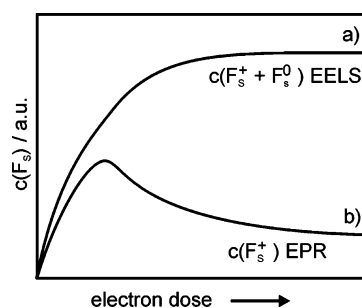


Figure 4. Schematic for the kinetics of color center formation on MgO thin films by electron bombardment obtained with (a) EELS¹² and (b) EPR (this study).

giving rise to an overall range of energy differences of 2.8 eV between 0.6 and 3.4 eV. The statistical analysis of these data shown in Figure 3b reveals a maximum occurrence of defects with an energy difference of 1.75–2 eV.

Discussion

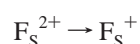
The EPR and STM data presented in Figures 1 and 2 give clear evidence that in the initial stages of electron bombardment of the MgO surface a substantial amount of F_s^+ centers are created, whereas, with increasing electron exposure times, also F_s^0 centers are formed and the concentration of F_s^+ centers partly decays. These results can qualitatively be compared to those of kinetic studies on the color center formation on MgO thin films performed with EELS.¹² From the electron-dosage-dependent evolution of the F_s EEL signals, the electron-induced color center formation was described by a first-order kinetics for F center formation and annihilation.¹² This model assumes that predominantly F_s^0 centers contribute to the EEL signal. Our results allow a more detailed view into the processes occurring on the surface as we selectively probe one charge state of color centers (F_s^+) with EPR, while in EELS the sum of F_s^+ and F_s^0 centers contributes to the signal intensity. In Figure 4, the experimental results for the kinetics of color center formation by electron bombardment obtained with EELS¹² and EPR are shown schematically. At variance with the simplified kinetic model used before, our results clearly prove the necessity to include the formation and annihilation of F_s^+ centers on the surface. In the following, we discuss possible mechanisms that lead to formation and annihilation of F_s^+ during electron bombardment of the MgO surface.

In terms of formation energies, the removal of a neutral oxygen atom, leaving behind two electrons trapped in an oxygen vacancy (F_s^0), is less costly than the formation of charged defects (F_s^+ , F_s^{2+}), which would justify the assumption made by Kramer et al. that only F_s^0 centers are formed during electron bombardment. However, the calculated formation energy of F_s^+ centers (10.8 eV) is only slightly higher than that of F_s^0 centers (9.3 eV).⁶ Taking into account that the energy of the impinging electrons is 100 eV, the energy of the final state is assumed to play only a minor role. It is more important to compare the energies and accessibilities of the transition states leading to the two different defect states to judge the branching ratio of the rates of formation. Unfortunately, almost nothing is known about them. From the experimental results we conclude, therefore, that during electron bombardment both F_s^+ and F_s^0 centers are created by electron-induced desorption. The observation of exclusively F_s^+ centers at low electron dosage in STM (Figure 2b) may be explained by electron trapping in preexisting trapping sites (F_s^{2+}), which are formed during the film growth. From STM images it can be seen that the step edges of the

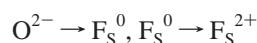
MgO islands are not perfectly straight but contain defects such as kinks, which, according to calculations, exhibit electron affinities comparable to those of bare oxygen vacancies. Therefore, in the regime of low electron dose, color centers are formed not only by electron-induced desorption but also by electron trapping on the surface, which, of course, depends on the surface defect density of the MgO film. Support for this suggestion comes from EPR experiments on freshly prepared versus annealed MgO films, where we find higher probabilities for color center formation on the freshly prepared than on the annealed film.

A third mechanism involving F_S^{2+} centers is their transformation into F_S^0 centers. At high electron dosage, the EPR results indicate a decay of F_S^{2+} centers, whereas a saturation concentration of F centers is observed with EELS.¹² It has to be considered, therefore, that although F_S^0 centers are the predominant surface defects after high electron exposure, their formation is only partly due to a direct process and an indirect route via capture of an electron by F_S^{2+} centers or tunneling recombination of F_S^{2+} centers to give F_S^0 centers is at least equally probable. Thus, the defect formation by electron bombardment includes at least the following microscopic steps:

(a) electron trapping in F_S^{2+}



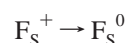
(b) formation and annihilation of F_S^0



(c) formation and annihilation of F_S^{+}



(d) transformation of F_S^{+} into F_S^0



Finally, there is a finite probability that color centers are destroyed by electron tunneling from the defect into the metallic substrate. Since this process seems to take place on a much longer time scale (hours), it can be ignored.

The formation probabilities of the individual defects are determined by several factors including the electronic properties of different color center species, diffusion constants (bulk-to-surface, surface-to-surface), and availability of sites. A number of experimental aspects such as the thickness of the MgO film, temperature, energy and geometry of electron bombardment, and influence of secondary electrons generated in the metallic substrate also have to be considered. The available experimental data do not allow for a detailed modeling of the processes occurring during electron bombardment, as has been shown, for example, for photoinduced excitation and desorption processes of KBr and MgO.²⁵ However, our results reveal that the processes involved in electron-assisted color center formation on the surface of MgO are more complex than previously assumed and show that a disentanglement of these processes is only possible by applying complementary spectroscopic methods that yield information on specific types of defects.

The electronic properties of color center defects on the MgO surface are well-known from theoretical calculations. In experiment, however, most spectroscopic results suffer from very

broad signals and the assignment of the spectral features to specific color center entities is difficult. For a detailed characterization of surface defects it is, therefore, desirable to obtain specific information with respect to the charge state and local environment. Regarding the local environment, a clear dependence of the electronic properties on the local coordination is expected from calculations.^{7,26} In a recent EELS study on color centers on a MgO film which was grown on a vicinal Ag(1,1,-19) substrate, Kramer et al. could isolate electronic excitations specific to color centers located on steps of MgO islands.¹³

The combination of low-temperature STM and STS has the prospect to determine the electronic states of defects, knowing their precise location. We have previously shown that F_S^{2+} centers located on one MgO facet show a clear correlation between the local environment and the energetic position of the electronic states, in agreement with theoretical predictions.^{7,16} Unfortunately, the extension of this approach to F_S^0 centers as shown in Figure 2d is not as straightforward. In particular, the apparent size of the features assigned to F_S^0 centers prevents a detailed determination of their location. From the STM images shown in Figure 2c,d it is difficult to judge whether defects located on terraces are single-ion vacancies or rather pits formed by desorption of a few MgO units where electrons are trapped at defects on the borders of the pits. Therefore, a distinct classification of the defects in terms of their local environment is difficult. The analysis of a large set of F_S^0 centers shown in Figure 3b indicates the variation of spectral data possible for these sites. The width of the distribution is determined not only by the existence of defects that are located on perfect terrace, step, or corner sites but also by the variable coordination in the second coordination sphere, which is evident from the STM images (Figure 2). Calculated electronic properties of trapped electrons in morphological sites such as divacancies, kinks, or reverse corners are very similar to those of color centers located at classical defect sites at terraces, steps, and corners. The electronic states of all existing defects are, therefore, expected to cover a wide range, which explains the large spread of the measured energy levels in Figure 3b. For the present case, it also has to be considered that the thickness of a nominally 4 ML thick MgO film may vary locally between 3 and 5 ML. In this ultrathin regime, the electronic interaction of a defect with the metallic substrate may to some extent vary with the thickness of the oxide layer and result in additional shifts of level energies. However, a systematic dependence on the thickness of the MgO film could not be established, indicating that this is not dominating the observed variations.

It is tempting to compare the measured energy difference of F_S^0 empty and filled states with the excitation energies of color centers on the MgO surface obtained from calculations and EELS experiments. The histogram in Figure 3b represents the occurrence of defects with a specific energy difference between empty and filled states derived from the tunneling spectra. The maximum occurrence found at around 2 eV is in agreement with the calculated singlet-to-singlet transition energy for color centers located at steps (1.9 eV)²⁶ and a prominent electron energy loss peak observed on MgO films grown on Ag(1,1,-19), which shows a dominance of step sites.¹³ Apart from defects located at steps, which are the majority species in our experiments, the existence of other defect sites exhibiting different coordinations (corners, kinks, terraces), as discussed above, are assumed to be responsible for the broad distribution of energy differences from 1 to 3.5 eV (Figure 3b). The occurrence of signals with broad envelopes that are generally observed for color centers with integrating spectroscopic techniques can,

therefore, be explained by the existence of a broad distribution of differently coordinated defect sites on the surface.

Conclusion

In summary, by a combination of EPR and STM experiments we have shown that singly charged color centers, F_S^+ , are produced during electron bombardment of MgO thin films and act as intermediate states for the formation of F_S^0 centers. The kinetics of color center formation by electron bombardment is, therefore, not only governed by the formation of F_S^0 centers but also has to be decomposed into contributions from both F_S^+ and F_S^0 defects. A broad distribution of ground-state energy levels of F_S^0 centers as detected by tunneling spectroscopy, as well as energy differences between unoccupied and occupied states, which can qualitatively be compared to calculated and measured excitation energies, is due to the different coordinations of the defects.

Electron bombardment of the MgO surface is a very efficient way to introduce surface defects with particular properties. In this paper we presented a modification of the model previously assumed for the formation of color centers by electron bombardment on the MgO surface, which was achieved by applying complementary spectroscopic and microscopic techniques. This is an important step toward understanding the mechanisms of defect creation, which is a necessary requirement for a specific modification of surface properties by defect engineering.

Acknowledgment. M.S. is grateful for financial support by the Austrian Science Fund (FWF). E.F. thanks the Studienstiftung des deutschen Volkes for financial support. This work was partially supported by the European Union through the STRP program GSOMEN and the NoE IDECAT.

References and Notes

- (1) Sterrer, M.; Yulikov, M.; Fischbach, E.; Heyde, M.; Rust, H.-P.; Pacchioni, G.; Risse, T.; Freund, H.-J. *Angew. Chem., Int. Ed.*, published online Mar 20, <http://dx.doi.org/10.1002/anie.200504443>.
- (2) Yoon, B.; Hakkinen, H.; Landman, U.; Worz, A. S.; Antonietti, J. M.; Abbet, S.; Judai, K.; Heiz, U. *Science* **2005**, *307*, 403.

- (3) Neyman, K. M.; Inntam, C.; Matveev, A. V.; Nasluzov, V. A.; Rösch, N. *J. Am. Chem. Soc.* **2005**, *127*, 11652.
- (4) Del Vitto, A.; Pacchioni, G.; Delbecq, F.; Sautet, P. *J. Phys. Chem. B* **2005**, *109*, 8040.
- (5) Pacchioni, G. *ChemPhysChem* **2003**, *4*, 1041.
- (6) Scorza, E.; Birkenheuer, U.; Pisani, C. *J. Chem. Phys.* **1997**, *107*, 9645.
- (7) Sushko, P. V.; Gavartin, J. L.; Shluger, A. L. *J. Phys. Chem. B* **2002**, *106*, 2269.
- (8) Ricci, D.; Di Valentin, C.; Pacchioni, G.; Sushko, P. V.; Shluger, A. L.; Giamello, E. *J. Am. Chem. Soc.* **2003**, *125*, 738.
- (9) Ricci, D.; Pacchioni, G.; Sushko, P. V.; Shluger, A. L. *J. Chem. Phys.* **2002**, *117*, 2844.
- (10) Chiesa, M.; Paganini, M. C.; Spoto, G.; Giamello, E.; Di Valentin, C.; Del Vitto, A.; Pacchioni, G. *J. Phys. Chem. B* **2005**, *109*, 7314.
- (11) Sterrer, M.; Stankic, S.; Diwald, O.; Knözinger, E. *ChemPhysChem* **2004**, *5*, 1695.
- (12) Kramer, J.; Ernst, W.; Tegenkamp, C.; Pfnür, H. *Surf. Sci.* **2002**, *517*, 87.
- (13) Kramer, J.; Tegenkamp, C.; Pfnür, H. *Phys. Rev. B* **2003**, *67*, 235401.
- (14) Kolmakov, A.; Stultz, J.; Goodman, D. W. *J. Chem. Phys.* **2000**, *113*, 7564.
- (15) Sterrer, M.; Fischbach, E.; Risse, T.; Freund, H.-J. *Phys. Rev. Lett.* **2005**, *94*, 186101.
- (16) Sterrer, M.; Heyde, M.; Novicki, M.; Nilius, N.; Risse, T.; Rust, H.-P.; Pacchioni, G.; Freund, H.-J. *J. Phys. Chem. B* **2006**, *110*, 46.
- (17) Wu, M.-C.; Corneille, J. S.; He, J.-W.; Estrada, C. A.; Goodman, D. W. *Chem. Phys. Lett.* **1991**, *182*, 472.
- (18) Gallagher, M. C.; Fyfield, M. S.; Bumm, L. A.; Cowin, J. P.; Joyce, S. A. *Thin Solid Films* **2003**, *445*, 90.
- (19) Schintke, S.; Messerli, S.; Pivetta, M.; Patthey, F.; Libiouille, L.; Stengel, M.; Vita, A. D.; Schneider, W.-D. *Phys. Rev. Lett.* **2001**, *87*, 276801.
- (20) Dohnálek, Z.; Kimmel, G. A.; Joyce, S. A.; Ayotte, P.; Smith, R. S.; Kay, B. D. *J. Phys. Chem. B* **2001**, *105*, 3747.
- (21) Sterrer, M.; Risse, T.; Freund, H. J. *Surf. Sci.* **2005**, *596*, 222.
- (22) Wu, M.-C.; Truong, C. M.; Goodman, D. W. *Phys. Rev. B* **1992**, *46*, 12688.
- (23) Di Valentin, C.; Neyman, K. M.; Risse, T.; Sterrer, M.; Fischbach, E.; Freund, H.-J.; Nasluzov, V. A.; Pacchioni, G.; Rösch, N. *J. Chem. Phys.*, in press.
- (24) Klaua, M.; Ullmann, D.; Barthel, J.; Wulfhekel, W.; Kirschner, J.; Urban, R.; Monchesky, T. L.; Enders, A.; Cochran, J. F.; Heinrich, B. *Phys. Rev. B* **2001**, *64*, 134411.
- (25) Hess, W. P.; Joly, A. G.; Beck, K. M.; Henyk, M.; Sushko, P. V.; Trevisanutto, P. E.; Shluger, A. L. *J. Phys. Chem. B* **2005**, *109*, 19563.
- (26) Sousa, C.; Pacchioni, G.; Illas, F. *Surf. Sci.* **1999**, *429*, 217.